Available online at www.sciencedirect.com
ScienceDirect
Catalysis Today 123 (2007) 198–207
CATALYSIS TODAY
www.elsevier.com/locate/cattod

# Hydrodesulfurization of 4,6-dimethyldibenzothiophene over Pt, Pd, and Pt–Pd catalysts supported on amorphous silica–alumina

Adeline Niquille-Röthlisberger, Roel Prins *

*Institute for Chemical and Bioengineering, ETH Zurich, 8093 Zurich, Switzerland*

Available online 27 February 2007

**Abstract**

The activities and selectivities of Pt, Pd, and Pt–Pd supported on amorphous silica–alumina (ASA) in the hydrodesulfurization (HDS) of 4,6-dimethyldibenzothiophene (4,6-DM-DBT) were investigated. The ASA-supported catalysts had much higher activities than alumina-supported catalysts, due to the creation of electron-deficient metal particles. Pd had a high hydrogenation activity for 4,6-DM-DBT, but the removal of sulfur from 4,6-DM-DBT and its HDS intermediates occurred faster over Pt than over Pd. Comparison of two Pt/ASA catalysts with different Pt loadings showed that the metal dispersion strongly influenced the product selectivity. Larger metal particles led to relatively faster hydrogenation and slower C–S bond breaking. Bimetallic Pt–Pd catalysts were much more active than the monometallic constituents, indicating that the metal particles were alloyed. Acid-catalyzed cracking and isomerization occurred especially over Pt/ASA.


*Keywords:* Hydrodesulfurization; 4,6-Dimethyldibenzothiophene; Dibenzothiophene; Platinum; Palladium; Pt–Pd catalysts; Amorphous silica–alumina

## 1. Introduction

In many countries legislation requires a very low sulfur content of transportation fuels. To attain this low level, also molecules such as 4,6-dimethyldibenzothiophene (4,6-DM-DBT), which are the most refractory molecules in deep hydrodesulfurization (HDS) technology [1–3], must be desulfurized. Because of steric hindrance by the methyl groups adjacent to the sulfur atom, the direct desulfurization of 4,6-DM-DBT to 3,3′-dimethylbiphenyl is almost completely suppressed and the HDS of 4,6-DM-DBT occurs predominantly by hydrogenation followed by desulfurization. Therefore, deep HDS is dependent on the hydrogenating ability of the catalyst. Metals are much better hydrogenation catalysts than metal sulfides and might, thus, be suited as catalysts for deep HDS. Unfortunately, metal particles transform into metal sulfide particles in the presence of sulfur-containing molecules, and metal sulfide particles are much less catalytically active than metal particles. The noble metals Pt and Pd are less susceptible to a transformation into inactive sulfides than other metals [4] and have been investigated for the removal of aromatic compounds from diesel fuel [5]. Because of their good hydrogenation properties, Pt and Pd are also good catalysts in HDS. The HDS of 4,6-DM-DBT is faster over Pd/γ-$Al_2O_3$ than over Pt/γ-$Al_2O_3$ and the combination of Pd and Pt greatly enhances the HDS activity and the hydrogenation properties of the alumina-supported catalyst [6].

Not only the noble metal, but also the support can improve the HDS activity of catalysts. Acidic supports, such as amorphous silica–alumina (ASA) and zeolites, increase the conversion of dibenzothiophene (DBT) [7] and of DBT substituted in the 4- and 6-position [7–11]. They enable dealkylation and isomerization reactions of the alkyl substituents, which may transform refractory components into more reactive species and thus accelerate HDS [7,11]. Acidic supports may also improve the catalytic activity of the catalyst particles. Partial electron transfer from the metal particles to the acidic sites of the support may explain this activity improvement, because the resulting electron-deficient metal particles [12–14] are said to have a better resistance to sulfur poisoning by decreasing the interaction with $H_2S$ [13,15]. Another explanation for the improved activity of metal particles on an acidic support is the creation of a second hydrogenation pathway by spillover of hydrogen atoms from the metal particles to the aromatic sulfur-containing molecules that are adsorbed on

* Corresponding author. Tel.: +41 44 6325490; fax: +41 44 6321162.
*E-mail address:* roel.prins@chem.ethz.ch (R. Prins).

0920-5861/$ – see front matter 
doi:10.1016/j.cattod.2007.01.053

acidic sites in the vicinity of the metal particles [16–18]. While the metal particles become poisoned by sulfur, they can still dissociate hydrogen molecules and the hydrogenation pathway by spillover would still be possible [19–21].

In this work we studied the HDS of 4,6-DM-DBT over Pt, Pd, and Pt–Pd catalysts supported on ASA. ASA is not as acidic as zeolites and the metal particles supported on ASA may not be as sulfur resistant as on a zeolite. On the other hand, metal particles on ASA may be less prone to catalyst deactivation by undesired side reactions such as cracking and coking, which lead to fast deactivation of zeolite-supported catalysts [22,23], and all metal particles in the mesopores of ASA are accessible to the reacting molecules. Therefore, we studied the influence of the ASA support on the network of HDS reactions of 4,6-DM-DBT, as well as the influence of the metal particle size.

## 2. Experimental

As support for the noble metals we used amorphous silica–alumina (ASA) obtained from Shell, which had a Si/Al ratio of 4.3, a surface area of 560 $m^2$/g, and a pore volume of 0.8 ml/g. The support was milled and sieved to 120–170 mesh size (90–125 μm), dried at 120 °C for 4 h, and calcined at 500 °C for 4 h. Pt and Pd were pore volume impregnated with aqueous solutions of $Pt(NH_3)_4(NO_3)_2$ (Aldrich, 99%) and $Pd(NH_3)_4(NO_3)_2$ (Alfa, 5 wt% solution), respectively. After impregnation, the catalysts were dried in air at room temperature for 3 h and then at 120 °C for 4 h, and finally calcined at 500 °C for 4 h (heating rate 5 °C/min). Monometallic 0.45 wt% Pt/ASA and 0.49 wt% Pd/ASA catalysts and a bimetallic 0.22 wt% Pt–0.25 wt% Pd/ASA catalyst were prepared and the metal loadings were determined by atomic absorption spectroscopy. These catalysts will be referred to hereafter as Pt/ASA, Pd/ASA, and Pt–Pd/ASA, respectively. The HDS of 4,6-DM-DBT was also investigated over another Pt/ASA catalyst, which had a higher metal loading of 1.9 wt% and was prepared by BP Amoco from Davison Grade 135 silica–alumina with a Si/Al ratio of 5.7. This catalyst will be referred to as Pt/ASA*. Hydrogen chemisorption was used to determine the dispersion of the metals on the support, as described before [6].

As the ASA-supported noble metal catalysts were very active, only 10 mg of catalyst was used in the catalytic experiments, diluted with SiC, and much lower weight times were needed to attain high conversion than over alumina-supported Pt and Pd catalysts [6]. The catalysts were reduced in situ in the microflow reactor and the HDS experiments with 4,6-DM-DBT (Acros, 95%) were performed at 300 °C and 5 MPa total pressure as described before for alumina-supported Pt, Pd, and Pt–Pd catalysts [6]. In short, every series of HDS experiments over a freshly in situ reduced noble metal catalyst started with a stabilization period of at least one night at the highest weight time (lowest flow rate), to diminish a possible influence of catalyst deactivation. Then, experimental data were collected with increasing flow rates of the sulfur feed and hydrogen (at constant ratio), thus with decreasing weight time. For each measuring point, we let the system stabilize for several hours (longer with low flow rates, shorter with high flow rates) after the change of flow conditions. We also checked for a possible deactivation of the catalysts by performing experiments with decreasing as well as increasing weight time. The difference in the conversion was only a few percent over the 2–3 weeks of the whole run with one catalyst. This means that stable conversions and selectivities were obtained after a few hours.

## 3. Results

### 3.1. Hydrogen chemisorption

After impregnation with the metal-containing solutions and drying, all ASA-supported catalysts had a BET surface area of 493–497 $m^2$/g. The metal dispersions were determined from the hydrogen chemisorption measurements carried out at 30 °C, between 0.1 and 2.0 kPa, and the strong $H_2$ adsorption was extrapolated to zero pressure to estimate the dispersion, assuming H/M = 1 at the metal surface. When hydrogen chemisorption measurements are carried out at such low hydrogen pressures and at 30 °C the formation of β-Pd hydride is avoided [24]. The corresponding metal particle sizes were calculated as indicated in [6]. The results are presented in Table 1. The dispersions of the Pt/ASA and Pt–Pd/ASA catalysts were equal (38%), while the dispersion of the Pd/ASA catalyst was higher (47%). These values are lower than the corresponding values (48–57%) of Pt, Pd, and Pt–Pd catalysts supported on γ-$Al_2O_3$ at the same metal loadings [6] and indicate that the metal particles are larger on the ASA than on the γ-$Al_2O_3$ support. The dispersion of the Pt/ASA* catalyst was lower (14%), in line with its four times higher metal loading than the Pt/ASA catalyst.

### 3.2. HDS over Pt/ASA

Five main types of products were observed in the HDS of 4,6-DM-DBT over Pt/ASA. Dimethylbiphenyl molecules (DM-BP) were observed as the product of the direct desulfurization (DDS) pathway, and dimethyltetrahydrodibenzothiophene molecules (DM-TH-DBT), dimethylhexahydrodibenzothiophene molecules (DM-HH-DBT), dimethylcyclohexylbenzene molecules (DM-CHB), and dimethylbicyclohexyl molecules (DM-BCH) as the intermediate and final products of the hydrogenation (HYD) route (Scheme 1). Fully hydrogenated sulfur-containing dimethylperhydrodibenzothiophene molecules (DM-PH-DBT) were only detected in trace amounts, probably because of fast desulfurization under the applied conditions.

Table 1
Metal dispersions and estimated particle sizes from strong hydrogen chemisorption measurements at 30 °C between 0.1 and 2.0 kPa

| Catalyst | Metal loading | | Dispersion (%) | Particle size (nm) |
|---|---|---|---|---|
| | Pt | Pd | | |
| Pt/ASA | 0.45 | | 38 | 3.5 |
| Pd/ASA | | 0.49 | 47 | 2.8 |
| Pt–Pd | 0.22 | 0.25 | 38 | 3.5 |
| Pt/ASA* | 1.9 | | 14 | 6.1 |

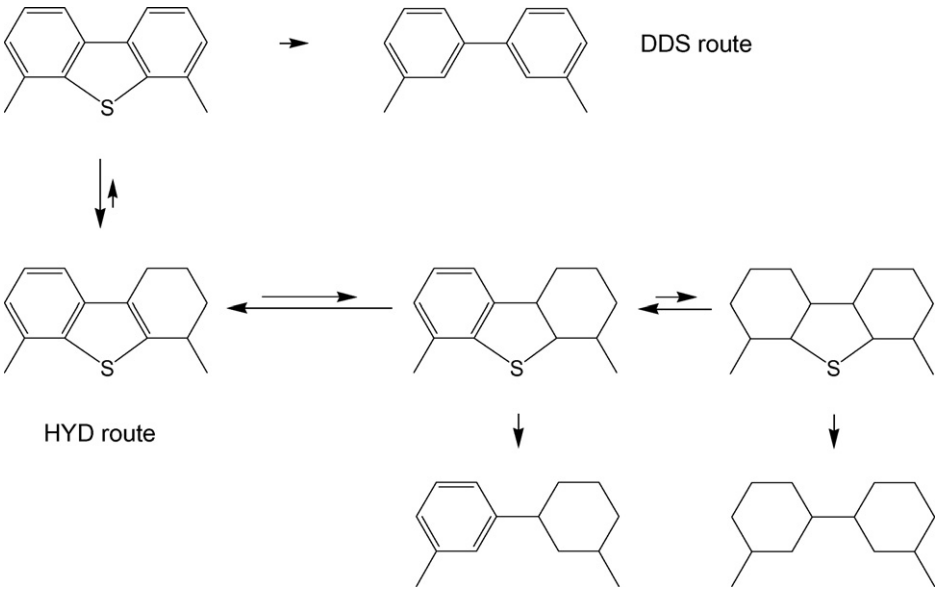


Scheme 1. Reaction network of the HDS of 4,6-DM-DBT over noble metal catalysts.

Because of the acidity of ASA, isomerization and cracking occurred. Isomers with methyl groups at positions different from those in 4,6-DM-DBT were observed for each product, but only a trace of an isomer of 4,6-DM-DBT itself was observed. The methyl shift, as well as the possibility of several isomers of the hydrogenated intermediates [25], led to numerous isomers. Each GC peak was quantified and analyzed by GC–MS to identify the main structure of the corresponding molecule, but it was not possible to fully characterize each molecule. To allow an overall analysis of the experimental results, the components were combined in separate classes. ''Expected products'' correspond to the sum of the reaction products that can be formed in the HDS of 4,6-DM-DBT without isomerization, as observed in the experiments over alumina-supported catalysts [6] and shown in Scheme 1. ''Isomerization products'' correspond to the sum of the products with the methyl groups at positions different from the 4- and 6-positions in the hydrogenated sulfur-containing intermediates (DM-TH-DBT and DM-HH-DBT in case of Pt/ASA) and from the 3 and 3′ positions in the desulfurized hydrocarbons (DM-CHB, DM-BCH, and DM-BP). ''Cracking products'' correspond to the cracking products toluene and methylcyclohexane, and the cracking yield is based on the percentage of 4,6-DM-DBT that transformed into cracked products. The overall yields and selectivities demonstrated that the amount of cracking depended on the metal. The cracked products reached a selectivity of 8% at high weight time over Pt/ASA (Fig. 1). An even larger amount of isomerized compounds was formed, leveling off at a selectivity of 32% at high weight time. Because of the cracking and isomerization, the selectivity of the ''expected products'' decreased with weight time. The selectivity of the expected products extrapolated to 100% with decreasing weight time. This means that the isomerization and cracking take place after the first hydrogenation reaction(s) and agrees with the fact that only a trace of an isomer of 4,6-DM-DBT was observed during reaction.

Fig. 2 presents the yields and selectivities of the reaction products in the HDS of 4,6-DM-DBT over Pt/ASA. All isomers of a product were lumped together under the same name. For instance, DM-TH-DBT is the sum of 4,6-DM-TH-DBT and all its isomers with the methyl groups at different positions. The cracking products, toluene and methylcyclohexane, are not

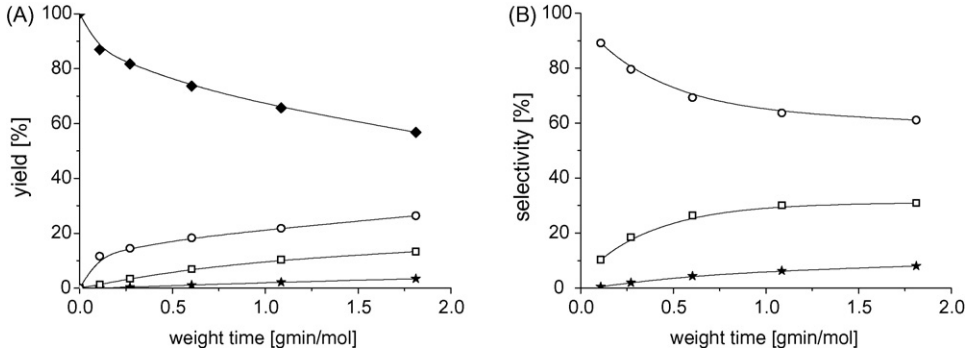


Fig. 1. Overall yields (A) and selectivities (B) in the HDS of 4,6-DM-DBT over Pt/ASA as a function of weight time (◆ 4,6-DM-DBT; ○ expected products; □ isomerization; ★ cracking).

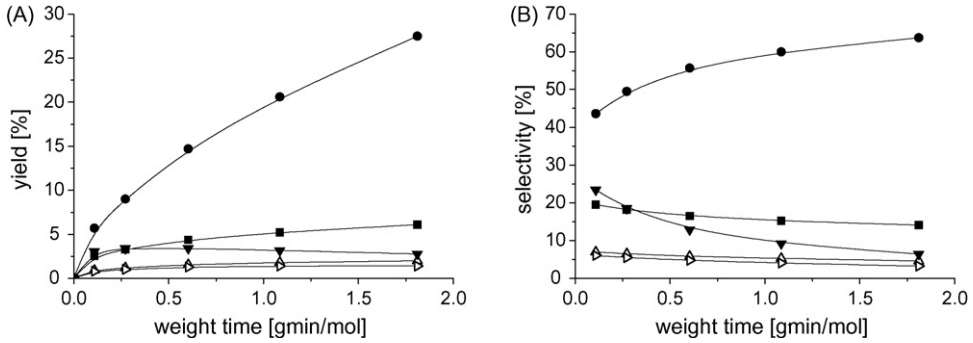


Fig. 2. Product yields (A) and selectivities (B) in the HDS of 4,6-DM-DBT over Pt/ASA as a function of weight time (△ DM-BP; ▼ DM-TH-DBT; ▷ DM-HH-DBT; ● DM-CHB; ■ DM-BCH).

represented in Fig. 2, to avoid overloading of the graphs, but they were included in the calculation of the product yields. DM-TH-DBT and DM-HH-DBT behaved like reaction intermediates, with yields passing through a maximum and selectivities decreasing continuously with weight time. The small amounts of sulfur-containing intermediates (with selectivities of 29% at low and 10% at high weight time) indicate that desulfurization over Pt/ASA is relatively easy. The major product in the HDS of 4,6-DM-DBT over Pt/ASA was DM-CHB at all times, while the second major product was DM-TH-DBT initially and DM-BCH at higher weight time. The selectivity of DM-CHB increased with weight time, while that of DM-BCH decreased slowly. Its decreasing selectivity indicates that DM-BCH reacts further by cracking to methylcyclohexane. Similarly, the decrease of the DM-BP selectivity from 7% at low weight time to 4.5% at high weight time points to cracking to toluene. Extrapolation of the DM-BP selectivity to $\tau = 0$ shows that 7.5% of 4,6-DM-DBT converted initially through the DDS route and 92.5% through the HYD pathway.

### 3.3. HDS over Pd/ASA

The Pd/ASA catalyst was much more active than Pt/ASA in the conversion of 4,6-DM-DBT, but cracking and isomerization were much lower than over Pt/ASA (cf. Figs. 1 and 3). The cracking selectivity reached only 0.2% and the isomerization selectivity reached 8% at high weight time. Six main products were observed, including DM-PH-DBT (Fig. 4). Much larger concentrations of sulfur components were observed over Pd/ASA than over Pt/ASA. They constituted 84% of the products at short weight time and still 45% at high weight time. This indicates that (partial) hydrogenation of 4,6-DM-DBT proceeds easily on Pd/ASA, but that the subsequent removal of sulfur is relatively difficult. The yields of DM-TH-DBT, DM-HH-DBT, and DM-PH-DBT passed through a maximum at $\tau \approx 0.4$, 0.4, and 0.9 g min/mol, respectively, while the selectivities of DM-TH-DBT and DM-HH-DBT decreased continuously and the selectivity of DM-PH-DBT showed a maximum at $\tau \approx 0.4$ g.min/mol. DM-TH-DBT and DM-HH-DBT seemed to evolve in parallel. Their ratio was constant throughout the reaction, suggesting a relatively fast equilibrium between these molecules. The fully hydrogenated sulfur-containing intermediate DM-PH-DBT behaved differently and had a higher yield than DM-HH-DBT above 0.2 g min/mol.

At low weight time DM-TH-DBT was the most abundant product but at higher weight time DM-BCH became the major product. DM-CHB and DM-BCH had steadily increasing yields and selectivities, suggesting that their further conversion was negligible. The DM-BCH to DM-CHB ratio was about 3.7, higher than the ratio of about 1.5 for $Pd/Al_2O_3$ [6]. The product of the DDS route, DM-BP, was only detected in trace amounts, meaning that 4,6-DM-DBT reacted almost exclusively (initially 99.9%) through the HYD pathway over Pd/ASA.

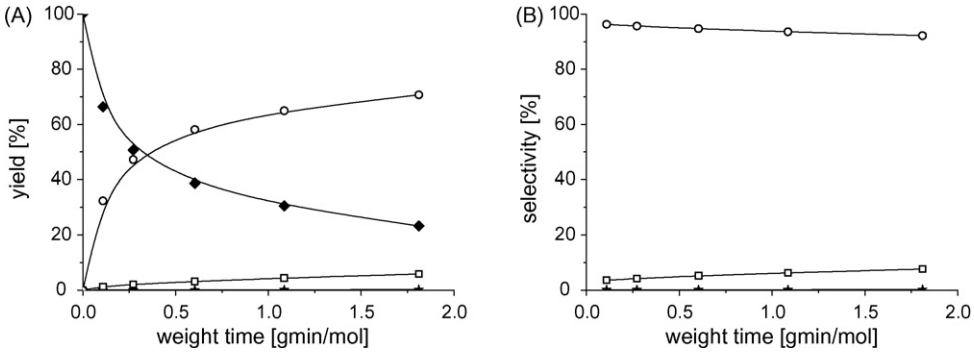


Fig. 3. Overall yields (A) and selectivities (B) in the HDS of 4,6-DM-DBT over Pd/ASA as a function of weight time (◆ 4,6-DM-DBT; ○ expected products; □ isomerization; ★ cracking).

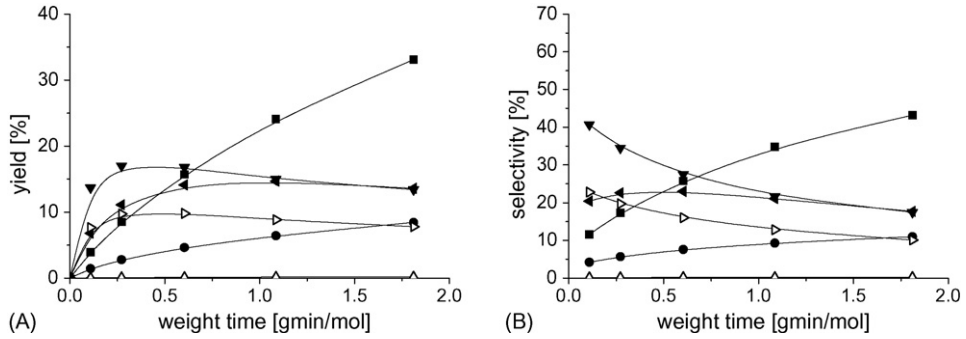


Fig. 4. Product yields (A) and selectivities (B) in the HDS of 4,6-DM-DBT over Pd/ASA as a function of weight time (△ DM-BP; ▼ DM-TH-DBT; ▷ DM-HH-DBT; ◀ DM-PH-DBT; ● DM-CHB; ■ DM-BCH).

### 3.4. HDS over Pt–Pd/ASA

As over Pd/ASA, cracking and isomerization were weak over Pt–Pd/ASA (0.2 and 6% selectivity at high weight time, respectively, not shown). Not only this overall product distribution, but also the product distribution of the six main reaction products over Pt–Pd/ASA was similar to that obtained over Pd/ASA (Fig. 5). DM-TH-DBT, DM-HH-DBT, and DM-PH-DBT represented 69% of the products at low and 21% at high weight time and their yields passed through a maximum at $\tau \approx 0.2$, 0.2, and 0.6 g min/mol, respectively. The selectivities of DM-TH-DBT and DM-HH-DBT decreased continuously with weight time, whereas that of DM-PH-DBT showed a maximum at $\tau \approx 0.3$ g min/mol. As over Pd/ASA, DM-TH-DBT and DM-HH-DBT evolved in parallel, with a constant ratio of 1.8 throughout the reaction. Again, DM-PH-DBT behaved differently; its yield was always higher than that of DM-HH-DBT and even higher than that of DM-TH-DBT above 0.4 g.min/mol.

Initially DM-TH-DBT was the major reaction product, while later DM-BCH became the most abundant product. It had a steadily increasing yield and selectivity and thus appeared to be a final product. DM-CHB was always the second major component and was present in higher concentration than DM-BCH at low weight time. Its selectivity leveled off at 27%. This suggests a subsequent conversion, probably by hydrogenation to DM-BCH, as cracking was negligible and isomerization was already taken into account in the product distribution. DM-BP was only observed in trace amounts. Its selectivity slightly decreased with weight time, suggesting that further hydrogenation occurred. Initially, 99.4% of 4,6-DM-DBT reacted via the HYD pathway and only 0.6% through the DDS route over Pt–Pd/ASA.

### 3.5. HDS over 1.9 wt% Pt/ASA*

The HDS of 4,6-DM-DBT was also investigated over a Pt catalyst with higher metal loading and lower dispersion in order to study the influence of the metal particle size on the reaction network. As over the Pt/ASA catalyst (0.45 wt% Pt), cracking was significant over the Pt/ASA* catalyst (1.9 wt% Pt) and reached a selectivity of 6% at high weight time (not shown). Large amounts of isomerization compounds were formed as well and at high weight time they constituted 33% of all reaction products. Because of these subsequent reactions of cracking and isomerization, the selectivity of the ‘‘expected products’’ decreased with weight time.

Five main products and traces of DM-PH-DBT were observed over Pt/ASA*. DM-TH-DBT and DM-HH-DBT behaved as intermediates, with yield passing through a maximum and selectivity decreasing with weight time. The major product up to $\tau = 0.8$ g min/mol, DM-TH-DBT, formed rapidly (Fig. 6). At higher weight time, the most abundant reaction component was DM-CHB and DM-BCH became the second main product at high weight time. Both products behaved as final products of the HYD pathway, with increasing yields and selectivities, as if further reactions did not take place. DM-BP formed slowly and its selectivity was practically constant at 1%. This suggests that

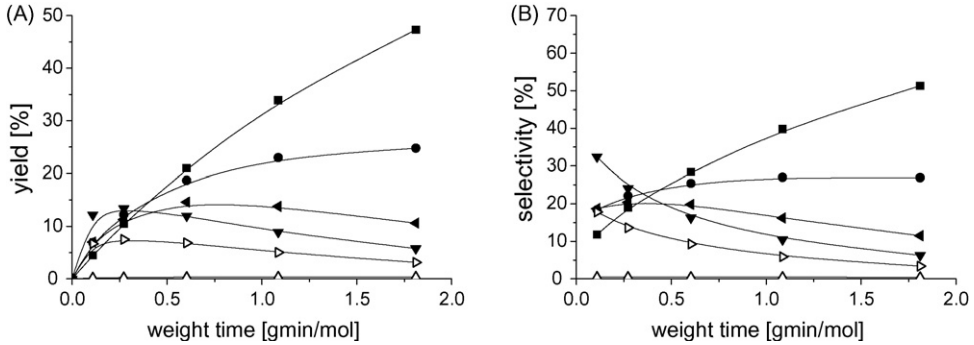


Fig. 5. Product yields (A) and selectivities (B) in the HDS of 4,6-DM-DBT over Pt–Pd/ASA as a function of weight time (△ DM-BP; ▼ DM-TH-DBT; ▷ DM-HH-DBT; ◀ DM-PH-DBT; ● DM-CHB; ■ DM-BCH).

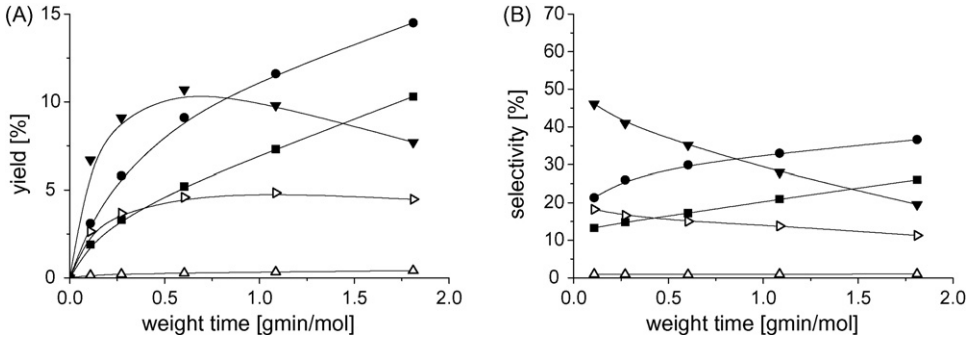


Fig. 6. Product yields (A) and selectivities (B) in the HDS of 4,6-DM-DBT over Pt/ASA* as a function of weight time (△ DM-BP; ▼ DM-TH-DBT; ▷ DM-HH-DBT; ● DM-CHB; ■ DM-BCH).

DM-BP did not hydrogenate further and means that the conversion of 4,6-DM-DBT over Pt/ASA* occurs 1% through the DDS route and 99% through the HYD pathway. The selectivities to sulfur-containing intermediates (64% at low and 31% at high weight time) were much higher than for Pt/ASA (29 and 10%, respectively) and indicate that desulfurization over Pt/ASA* is relatively slower than over Pt/ASA.

## 4. Discussion

### 4.1. ASA-supported noble metal catalysts

The reactivity of the metal catalysts supported on ASA followed the order Pt–Pd > Pd > Pt (Fig. 7A), the same as on $Al_2O_3$ [6,26]. The activity differences were not caused by differences in metal particle size, as all catalysts had similar dispersions (Table 1). Assuming pseudo-first-order kinetics for the reaction of 4,6-DM-DBT at low conversion (low weight time), rate constants $k$ were calculated for all catalysts (Table 2). They showed that Pd/ASA is almost three times more active than Pt/ASA and that the combination of Pt and Pd further increases the activity by 15% at the same total metal loading (≈0.5 wt%). When the molar weights and the dispersions are taken into account, the resulting turnover frequencies (TOF) showed that 4,6-DM-DBT converts 20% faster over Pd/ASA than over Pt/ASA and almost twice as fast over Pt–Pd/ASA as over Pd/ASA (Table 2).

The initial selectivity of the DDS pathway in the HDS of 4,6-DM-DBT over the ASA-supported catalysts was highest for Pt/ASA (7.5%), but lower than for the Pt/γ-$Al_2O_3$ catalyst (15%) (Table 2). All Pd-containing catalysts converted 4,6-DM-DBT almost exclusively through the HYD route (≥99%). The Pt–Pd/ASA catalyst behaved very similarly to Pd/ASA, which indicates that its surface properties are very close to those of Pd/ASA [27], most probably due to Pd segregation on the catalyst surface [28]. The initial $TOF_{DDS}$ and $TOF_{HYD}$ for the DDS and HYD reaction pathways, respectively, calculated from the initial selectivities of these two pathways and the turnover frequencies TOF, show that Pt/ASA is 55 times faster and Pt–Pd/ASA 10 times faster than Pd/ASA in the DDS pathway. More important than the $TOF_{DDS}$ values are, however, the much higher $TOF_{HYD}$ values and of these the $TOF_{HYD}$ for Pd/ASA is 30% higher and that for Pt–Pd/ASA 140% higher than for Pt/ASA (Table 2). These results are in good agreement with the higher conversion observed in the HDS of 4-ethyl-6-methyl-DBT (4-E-6-M-DBT) over Pd/ASA than over Pt/ASA [7], and the even higher conversion of 4-E-6-M-DBT [9,29] and DBT [9] over Pt–Pd/ASA.

Because of the good desulfurization ability of Pt/ASA, the conversion to desulfurized products (HDS conversion) was only slightly smaller than the total conversion of 4,6-DM-DBT (cf. Fig. 7A and B). On the contrary, over Pd/ASA and Pt–Pd/ASA the total and HDS conversions differed substantially, and thus the three sulfur-containing intermediates represented a

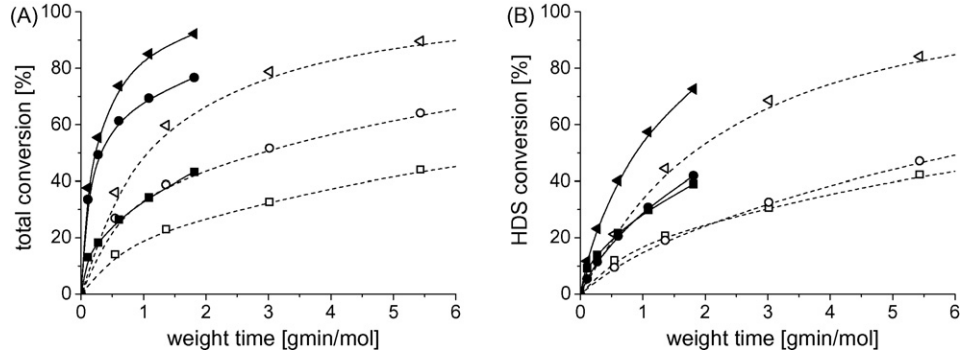


Fig. 7. Total conversion (A) and HDS conversion (B) in the HDS of 4,6-DM-DBT over different supported noble metal catalysts (□ Pt/γ-$Al_2O_3$; ○ Pd/γ-$Al_2O_3$; ◁ Pt–Pd/γ-$Al_2O_3$; ■ Pt/ASA; ● Pd/ASA; ◀ Pt–Pd/ASA).

Table 2
Pseudo first-order rate constants ($k$ in mol/min $g_{cat}$), initial selectivities ($S$ in %), and turnover frequencies (TOF in mol/min mmol) for the conversion of 4,6-DM-DBT over ASA-supported and alumina-supported [6] noble metal catalysts

| Catalyst | $k$ | $S_{HYD}$ | $S_{DDS}$ | TOF | $TOF_{HYD}$ | $TOF_{DDS}$ |
|---|---|---|---|---|---|---|
| Pt/ASA | 1.28 | 92.5 | 7.5 | 146 | 135 | 11 |
| Pd/ASA | 3.76 | 99.9 | 0.1 | 174 | 174 | 0.2 |
| Pt–Pd/ASA | 4.34 | 99.4 | 0.6 | 329 | 327 | 2 |
| Pt/ASA* | 1.44 | 99.0 | 1.0 | 106 | 105 | 1 |
| Pt/γ-$Al_2O_3$ | 0.28 | 85 | 15 | 18 | 15 | 3 |
| Pd/γ-$Al_2O_3$ | 0.58 | 99 | 1 | 22 | 22 | 0.2 |
| Pt–Pd/γ-$Al_2O_3$ | 0.83 | 99 | 1 | 46 | 45 | 0.5 |

large part of the 4,6-DM-DBT conversion. For instance, at 40% conversion the selectivity to the three sulfur-containing intermediates was 81% for Pd/ASA, 67% for Pt–Pd/ASA, and only 11% for Pt/ASA.

The higher HYD selectivity and higher selectivity to sulfur-containing intermediates for Pd/ASA than for Pt/ASA indicate that the hydrogenation steps are rather easy on the Pd surface but that the removal of sulfur is relatively difficult. Also, DM-TH-DBT and DM-HH-DBT were found to be in fast equilibrium over Pd/ASA, indicating that hydrogenation and dehydrogenation reactions between these two molecules are not rate limiting. Furthermore, 4,6-DM-DBT reacted mainly to DM-BCH over Pd/ASA but to DM-CHB over Pt/ASA and only a trace amount of the fully hydrogenated DM-PH-DBT was observed over Pt/ASA. This confirms the good hydrogenation properties of Pd, leading to the fast formation of large amounts of DM-PH-DBT and a rather slow desulfurization to DM-BCH (cf. Scheme 1). Pt, on the other hand, had a relatively high desulfurization ability and converted DM-HH-DBT rapidly to DM-CHB. These results agree with observations that Pd had a higher activity than Pt in the hydrogenation of small aromatic hydrocarbons in the presence of sulfur components [10,30–34] and in the HDS of substituted dibenzothiophene derivatives in a straight-run light gasoil [26] and of 4-E-6-M-DBT in a model reaction [7]. Similarly, Pd catalysts showed a much higher ratio of 3,3′-DM-BCH to 3,3′-DM-CHB than Pt in the HDS of 4,6-DM-DBT [10].

The bimetallic catalyst had the highest activity of the ASA-supported catalysts in the HDS of 4,6-DM-DBT and did not show intermediate properties between those of Pt and Pd. This demonstrates the occurrence of a chemical synergism and the presence of active sites of a new type (with different electronic and/or geometrical characteristics) due to the alloying of Pd with Pt. Synergetic effects were also observed in the HDS of thiophene [35], DBT [32], 4-E-6-M-DBT [8,9,29], and a straight-run gasoil [26,29,36]. The combination of Pd and Pt also greatly accelerated the hydrogenation of small aromatic hydrocarbons in the presence of sulfur-containing compounds [36–39]. The behavior of our Pt–Pd/ASA catalyst in the HDS of 4,6-DM-DBT was very similar to that of the monometallic Pd/ASA catalyst, with a very high HYD selectivity, a high selectivity to sulfur-containing intermediates, a constant ratio of DM-TH-DBT to DM-HH-DBT, and DM-BCH as the main desulfurized product. Over Pt–Pd/ASA, the partial pressure of DM-PH-DBT was higher than of DM-HH-DBT throughout the reaction and higher than of DM-TH-DBT above 0.4 g min/mol. The $TOF_{HYD}$ was 1.9 times larger over Pt–Pd/ASA than over Pd/ASA. All these results demonstrate that the Pt–Pd catalyst has very good hydrogenation properties and that new active sites must be present with excellent hydrogenation ability.

An EXAFS investigation of Fujikawa et al. indicated that Pd and Pt were alloyed in Pt–Pd catalysts. They proposed that this explains the enhanced catalytic activity for the hydrogenation of aromatics in distillates [5,38]. The bimetallic Pt–Pd system is known to be strongly surface enriched in Pd [28]. For our Pt–Pd catalyst, with a molar ratio of about Pd/Pt = 2 and a metal dispersion of 38%, complete phase segregation would mean that the two outermost metal layers consist completely of Pd atoms, surrounding a Pt kernel. How the underlying Pt atoms then influence the properties of the surface Pd atoms is not clear. On the other hand, segregation is known to be less strong in small metal particles and at elevated temperature. Furthermore, theoretical studies of other metal overlayer structures indicate that lattice mismatch as well as electronic interactions can influence the electronic properties of the surface atoms [40]. Lattice mismatch leads to changes in the Pd–Pd distance and bonding, which in turn changes the adsorbate–Pd interaction. When this weakens the interaction between sulfur and Pd atoms, it may improve the sulfur tolerance of the bimetallic catalyst [41]. Hence, alloying prevents the sulfur poisoning responsible for the decrease in the metal–support interaction and of the promotion of Pt migration [42,43]; it avoids the growth of particle size and, therefore, the loss of active metal surface, and leads to an enhanced performance in respect to the monometallic catalysts.

### 4.2. Influence of the support

The activity of the ASA-supported catalysts in the HDS of 4,6-DM-DBT was much higher (7–8 times) than that of the corresponding alumina-supported catalysts, as shown by the conversions in Fig. 7 and the rate constants and turnover frequencies in Table 2. The same activity order, Pt–Pd > Pd > Pt, was found on both supports. A positive influence of acid supports has been observed in many areas of catalysis. For instance, the hydrogenolysis of neopentane was faster over Pd supported on a zeolite than on alumina [44], small aromatic hydrocarbons were hydrogenated faster with increasing acidity of the support [10,16–21,30,31,33,37,45–47], and the HDS activity of Pt [7,9] and transition-metal sulfide catalysts increased with increasing support acidity [11,22,48–54].

The support effect can be explained in several ways: (i) by a higher dispersion of the catalyst particles on the support, (ii) by a new catalytic mechanism, or (iii) by changes in the catalytic properties of the metal particles. The first explanation does not seem likely, because the dispersion of the noble metal particles on ASA was lower than on alumina. The second explanation, new catalytic reaction paths, may be possible if the steric hindrance by the methyl groups in the 4- and 6-positions were removed [7]. This may occur by dealkylation, transalkylation, and isomerization of 4,6-DM-DBT over an acidic Pt catalyst.

These reactions have been observed in the HDS of metal sulfide catalysts supported on acid zeolite HY at 340 °C and they indeed contributed greatly to the increased catalytic activity [11,50]. Cracking and isomerization were much less important at 280 °C for a sulfided NiW catalyst supported on a less acidic mesoporous aluminosilicate, assembled from beta-zeolite seeds [55]. Our cracking and isomerization results, obtained at 300 °C, were between the HY and mesoporous aluminosilicate results. Nevertheless, dealkylation cannot explain the higher activity of our ASA-supported catalysts compared with the alumina-supported catalysts, because neither methyl-DBT, nor DBT, nor any of their corresponding HDS derivatives were detected at 300 °C. Isomerization of intermediates and final products as well as cracking took place, but their yields cannot explain the higher conversions over the ASA-supported catalysts, because the concentrations of the isomerized intermediates were only moderate for Pt/ASA and of minor importance for the Pd/ASA and Pt–Pd/ASA catalysts. Another new reaction that might take place is hydrogenation by spillover of hydrogen atoms to 4,6-DM-DBT molecules adsorbed on the support in the vicinity of the metal particles. Lin and Vannice proposed this pathway to explain the faster hydrogenation of benzene and toluene over Pt and Pd catalysts supported on acid supports [16,17]. Simon et al. used the same explanation for the hydrogenation of benzene in the presence of thiophene [19–21]. They proposed that $H_2S$, which is formed from thiophene, poisons the benzene hydrogenation over the metal surface, but that hydrogen molecules can still dissociate on the sulfided metal surface. The resulting hydrogen atoms can spillover to the support and hydrogenate benzene molecules that are adsorbed on acid sites in the vicinity of the metal particles.

The third explanation for the enhancement of the catalyst activity with increasing support acidity is partial electron transfer from the noble metal particles to the acidic sites on the support [13,44,56]. Della Betta and Boudart were the first to propose that the removal of electrons from antibonding orbitals increases the bonding properties and thus the catalytic activity of the noble metal particles [56]. For reactions in the presence of sulfur, such as HDS reactions, it has been proposed that the electron-deficient noble metal particles bind the electron-acceptor sulfur atoms weaker. As a consequence, there are more sulfur vacancies on the surface of metal particles in contact with acid sites of ASA and these vacancies act as the catalytic sites [57]. The weaker sulfur–metal interaction also makes the metal particles more resistant to sulfur poisoning [13,15]. Therefore, the metal–support interaction remains strong, the agglomeration of the noble metal particles is prevented, and the dispersion and catalytic activity remain high. Very small Pt particles have a higher sulfur resistance because of their better contact with the acidic support, leading to a more pronounced electron-deficient character [13,27,45]. An increase in the particle size decreases the sulfur tolerance of Pt and Pd supported on high-silica zeolite [58]. However, the sulfur tolerance was more sensitive to the acidity of the support than to the particle size of Pt clusters [13,59]. This agrees with our hydrogen chemisorption measurements, which showed that the metal particles on ASA are about 50% larger than on alumina [6]. Nevertheless, the activity of the ASA-supported catalysts in the HDS of 4,6-DM-DBT was much higher than that of the alumina-supported catalysts (Table 2), confirming the dominant influence of the support acidity. Table 2 shows that alloying and the acid support both improve the catalytic activity, but that the improvement in the reactivity of 4,6-DM-DBT over Pt–Pd/ASA comes mainly from the modification of the properties of the noble metal active sites by the support acidity. The change in the electronic properties of the metal particles induced by the acid sites explains why the hydrogenolysis of neopentane, the hydrogenation of aromatic hydrocarbons, and the HDS of 4,6-DM-DBT are all positively influenced by support acidity. Otherwise it would be difficult to understand why the acidic support would influence the neutral neopentane molecule.

### 4.3. Influence of the metal particle size

All three metal catalysts (Pt, Pd, and Pt–Pd) showed relatively faster hydrogenation and slower C–S bond breaking when supported on ASA than on alumina. Thus, all M/ASA catalysts had higher DM-TH-DBT and DM-HH-DBT selectivities and a lower DM-BP selectivity than the corresponding M/$\gamma$-$Al_2O_3$ catalysts. The ratio DM-BCH to DM-BCH was higher over M/ASA than over M/$\gamma$-$Al_2O_3$ catalysts and Pd and Pt–Pd on ASA had a high selectivity to DM-PH-DBT. The same trend, relatively more hydrogenation and less C–S bond breaking, was also apparent for Pt/ASA* relative to Pt/ASA. Pt/ASA* had the highest HYD selectivity of all three Pt catalysts investigated and the lowest $TOF_{DDS}$ value (Table 2). The DM-BCH to DM-CHB ratio for Pt/ASA* was 0.7 at high weight time, rather than 0.2 for Pt/ASA. The selectivities of the sulfur-containing intermediates at constant conversion (35%) were 42% over Pt/ASA*, 13% over Pt/ASA, and 6% over Pt/$\gamma$-$Al_2O_3$. All these facts indicate that the ratio of hydrogenation (of 4,6-DM-DBT to the intermediates) to desulfurization (of the intermediates to hydrocarbons) was highest for Pt/ASA*.

While the alumina- and ASA-supported metal catalysts differ in support acidity as well as metal dispersion, the Pt/ASA and Pt/ASA* catalysts have similar Al contents (19 and 15%, respectively) and are therefore expected to have similar support acidity. We checked by MAS-NMR that the fraction of tetrahedral Al sites (which are responsible for the acidity of ASA) in both ASA supports was indeed similar. The similar acidity of ASA and ASA* enables a direct comparison of the effect of Pt particle size. The larger particle size of the metal particles in the Pt/ASA* catalyst might explain why the DM-BP selectivity was lower and the selectivities to the sulfur-containing intermediates were higher than for the Pt/ASA catalyst. Larger metal particles have relatively less edge and kink sites and more sites in low-index planes. This disfavors hydrogenolysis and relatively favors hydrogenation reactions, because the DDS route needs $\sigma$ adsorption on one active site through the sulfur atom of the reactant, whereas the HYD pathway in the HDS of 4,6-DM-DBT most probably occurs by $\pi$ adsorption of the molecule on several metal atoms. The lower dispersions of Pt, Pd, and Pt–Pd on ASA (38–47%) than on alumina (48–57%) can also explain the selectivity differences

between the ASA- and alumina-supported catalysts. Another explanation for the differences in activity and selectivity between Pt/ASA and Pt/ASA* could be that the effect of the acidic support is weaker for the larger Pt particles in Pt/ASA*. However, the $TOF_{HYD}$ of Pt/ASA* is only 22% smaller than that of Pt/ASA and still very much larger than that of Pt/γ-$Al_2O_3$.

The higher DDS selectivity of the Pt than of the Pd catalysts may be due to a higher tolerance to $H_2S$. In the HDS of 4,6-DM-DBT over $MoS_2$ and Co and Ni-promoted $MoS_2$ catalysts, $H_2S$ inhibited the DDS route more than the HYD route [60]. The same may happen on the Pt and Pd catalysts. Because the methyl groups strongly hinder the interaction of the sulfur lone pair with the metal atom on the catalyst surface in the $\sigma$ adsorption mode, only exposed metal atoms will be able to catalyze DDS. Exposed metal atoms at kinks and edges have fewer neighbors than metal atoms in low index planes and should be more susceptible to sulfur poisoning. The observation that in all cases the alumina-supported noble metals had a higher DDS selectivity (Table 2) can be explained by their higher dispersion and thus higher fraction of exposed metal atoms.

The cracking and isomerization was much higher over Pt/ASA than over Pd/ASA and Pt–Pd/ASA. Since these reactions did not take place on the corresponding metal catalysts supported on alumina [6], they must take place on the acidic sites on the ASA support. The explanation why the metal has such a large effect may be indirect. For instance, if the spillover of hydrogen atoms from the metal particles to the ASA support is more extensive for the Pt/ASA catalyst than for the Pd-based catalysts, there will be less coke formation by oligomerization reactions on the acid sites and less deactivation of the acid-catalyzed cracking and isomerization reactions.

The $TOF_{HYD}$ and $TOF_{DDS}$ are higher for the ASA-supported catalysts than for the alumina-supported ones, but the $TOF_{HYD}$ is more enhanced than the $TOF_{DDS}$ (Table 2). If we assume that the C–S bond breaking in the hydrogenated intermediates correlates with the C–S bond breaking in 4,6-DM-DBT (thus with $TOF_{DDS}$), we can understand that the difference between the total conversion and the HDS conversion curves is larger for the ASA-supported catalysts than for the γ-$Al_2O_3$-supported catalysts (Fig. 7), because over ASA the desulfurization cannot keep pace with the much faster hydrogenation. Since this is most obvious over Pd, it explains why the fully hydrogenated sulfur-containing intermediate DM-PH-DBT could only be detected on the Pd-based catalysts, and why DM-BCH was the major reaction product over Pd and DM-CHB over Pt.

## 5. Conclusions

ASA-supported Pt, Pd, and Pt–Pd catalysts were much more active than the corresponding alumina-supported catalysts in the HDS of 4,6-DM-DBT and the support acidity had a similar influence on all catalysts. Thus, as on alumina, Pt was a better desulfurization catalyst than Pd, and Pd had better hydrogenation properties. The bimetallic Pt–Pd catalyst showed an outstanding HDS performance and a product distribution close to that of Pd, indicating the occurrence of chemical synergism between Pt and Pd and the existence of surface Pd enrichment. The greater enhancement of the HYD pathway may be due to the presence of new active sites with improved hydrogenation properties. The Pt catalyst with larger particles had a higher hydrogenation selectivity than the one with smaller Pt particles. A possible explanation is that hydrogenation requires large ensembles of active sites, such as terraces, for the $\pi$ adsorption of the reactants, which is proportionally enhanced by the particle growth.

Isomerization and cracking reactions could not explain the improvement of the activity occurring on the surface of our acidic catalysts. Electron-deficient metal particles that arise from a partial charge transfer from the metal clusters to the acidic sites of the support can explain that the adsorption of $H_2S$ is inhibited, leading to a better sulfur resistance and to higher hydrogenation properties. When acidic supports improve the HDS activity of noble metal catalysts substantially it would be logical to use zeolites as support, because of their higher acidity than ASA. A drawback of zeolites is, however, that their pores are too small to give access to molecules like dialkylated-DBT. The catalytic reaction is then restricted to catalyst particles on the outer surface. Another drawback is their fast deactivation by coke formation on the acid sites by alkenes and dienes formed by dehydrogenation on the metal [22,23,57].

## References

[1] M.J. Girgis, B.C. Gates, Ind. Eng. Chem. Res. 30 (1991) 2021.
[2] D.D. Whitehurst, T. Isoda, I. Mochida, Adv. Catal. 42 (1998) 345.
[3] T. Kabe, A. Ishihara, W. Qian, Hydrodesulfurization and Hydrodenitrogenation, Wiley–VCH, Weinheim, 1999.
[4] T.A. Pecoraro, R.R. Chianelli, J. Catal. 67 (1981) 430.
[5] T. Fujikawa, K. Idei, T. Ebihara, H. Mizuguchi, K. Usui, Appl. Catal. A 192 (2000) 253.
[6] A. Niquille-Röthlisberger, R. Prins, J. Catal. 242 (2006) 207.
[7] W. Robinson, J.A.R. van Veen, V.H.J. de Beer, R.A. van Santen, Fuel Process. Technol. 61 (1999) 103.
[8] H.R. Reinhoudt, R. Troost, S. van Schalkwijk, A.D. van Langeveld, S.T. Sie, H. Schulz, D. Chadwick, J. Cambra, V.H.J. de Beer, J.A.R. van Veen, J.L.G. Fierro, J.A. Moulijn, Stud. Surf. Sci. Catal. 106 (1997) 237.
[9] H.R. Reinhoudt, R. Troost, A.D. van Langeveld, J.A.R. van Veen, S.T. Sie, J.A. Moulijn, Stud. Surf. Sci. Catal. 127 (1999) 251.
[10] T. Matsui, M. Harada, M. Toba, Y. Yoshimura, Appl. Catal. A-Gen. 293 (2005) 137.
[11] F. Bataille, J.L. Lemberton, G. Perot, P. Leyrit, T. Cseri, N. Marchal, S. Kasztelan, Appl. Catal. A 220 (2001) 191.
[12] F. Figueras, B. Mencier, L. De Mourgues, C. Naccache, Y. Trambouze, J. Catal. 19 (1970) 315.
[13] P. Gallezot, Catal. Rev. Sci. Eng. 20 (1979) 121.
[14] W.M.H. Sachtler, A.Y. Stakheev, Catal. Today 12 (1992) 283.
[15] B.H. Cooper, B.B.L. Donnis, Appl. Catal. A 137 (1996) 203.
[16] S.D. Lin, M.A. Vannice, J. Catal. 143 (1993) 539.
[17] S.D. Lin, M.A. Vannice, J. Catal. 143 (1993) 563.
[18] S.D. Lin, M.A. Vannice, J. Catal. 143 (1993) 554.
[19] L.J. Simon, J.G. van Ommen, A. Jentys, J.A. Lercher, J. Phys. Chem. B 104 (2000) 11644.
[20] L.J. Simon, J.G. van Ommen, A. Jentys, J.A. Lercher, J. Catal. 201 (2001) 60.
[21] L.J. Simon, J.G. van Ommen, A. Jentys, J.A. Lercher, J. Catal. 203 (2001) 434.
[22] W.J.J. Welters, V.H.J. de Beer, R.A. van Santen, Appl. Catal. A 119 (1994) 253.

[23] R. Navarro, B. Pawelec, J.L.G. Fierro, P.T. Vasudevan, J.F. Cambra, M.B. Guemez, P.L. Arias, Fuel Process. Technol. 61 (1999) 73.
[24] V. Ragaini, R. Giannantonio, P. Magni, L. Lucarelli, G. Leofanti, J. Catal. 146 (1994) 116.
[25] P. Kukula, V. Gramlich, R. Prins, Helv. Chim. Acta 89 (2006) 1623.
[26] A. Ishihara, F. Dumeignil, J. Lee, K. Mitsuhashi, E.W. Qian, T. Kabe, Appl. Catal. A 289 (2005) 163.
[27] T. Matsui, M. Harada, K.K. Bando, M. Toba, Y. Yoshimura, Appl. Catal. A 290 (2005) 73.
[28] L.D. Lloyd, R.L. Johnston, S. Salhi, N.T. Wilson, J. Mater. Chem. 14 (2004) 1691.
[29] H.R. Reinhoudt, R. Troost, A.D. van Langeveld, S.T. Sie, J.A.R. van Veen, J.A. Moulijn, Fuel Process. Technol. 61 (1999) 133.
[30] R.M. Navarro, B. Pawelec, J.M. Trejo, R. Mariscal, J.L.G. Fierro, J. Catal. 189 (2000) 184.
[31] H. Yasuda, Y. Yoshimura, Catal. Lett. 46 (1997) 43.
[32] J.L. Rousset, L. Stievano, F. Aires, C. Geantet, A.J. Renouprez, M. Pellarin, J. Catal. 202 (2001) 163.
[33] C.S. Song, A.D. Schmitz, Energy Fuels 11 (1997) 656.
[34] W. Qian, Y. Yoda, Y. Hirai, A. Ishihara, T. Kabe, Appl. Catal. A-Gen. 184 (1999) 81.
[35] M. Sugioka, F. Sado, Y. Matsumoto, N. Maesaki, Catal. Today 29 (1996) 255.
[36] T.B. Lin, C.A. Jan, J.R. Chang, Ind. Eng. Chem. Res. 34 (1995) 4284.
[37] B. Pawelec, R. Mariscal, R.M. Navarro, S. van Bokhorst, S. Rojas, J.L.G. Fierro, Appl. Catal. A 225 (2002) 223.
[38] T. Fujikawa, K. Tsuji, H. Mizuguchi, H. Godo, K. Idei, K. Usui, Catal. Lett. 63 (1999) 27.
[39] S. Albonetti, G. Baldi, A. Bazzanti, E. Rodriguez Castellon, A. Jimenez Lopez, D. Eliche Quesada, A. Vaccari, Catal. Lett. 108 (2006) 197.
[40] A. Gross, Topics Catal. 37 (2006) 29.
[41] N. Matsubayashi, H. Yasuda, M. Imamura, Y. Yoshimura, Catal. Today 45 (1998) 375.
[42] M. Vaarkamp, J.T. Miller, F.S. Modica, G.S. Lane, D.C. Koningsberger, J. Catal. 138 (1992) 675.
[43] J.R. Chang, S.L. Chang, T.B. Lin, J. Catal. 169 (1997) 338.
[44] S.T. Homeyer, Z. Karpinski, W.M.H. Sachtler, J. Catal. 123 (1990) 60.
[45] A. Corma, A. Martinez, V. Martinez-Soria, J. Catal. 169 (1997) 480.
[46] K. Thomas, C. Binet, T. Chevreau, D. Cornet, J.P. Gilson, J. Catal. 212 (2002) 63.
[47] H. Yasuda, T. Sato, Y. Yoshimura, Catal. Today 50 (1999) 63.
[48] R. Cid, J. Neira, J. Godoy, J.M. Palacios, S. Mendioroz, A. Lopez Agudo, J. Catal. 141 (1993) 206.
[49] E.J.M. Hensen, V. de Beer, J.A.R. van Veen, R.A. van Santen, J. Catal. 215 (2003) 353.
[50] P. Michaud, J.L. Lemberton, G. Perot, Appl. Catal. A 169 (1998) 343.
[51] T. Isoda, S. Nagao, X.L. Ma, Y. Korai, I. Mochida, Energy Fuels 10 (1996) 1078.
[52] M. Yumoto, K. Usui, K. Watanabe, K. Idei, H. Yamazaki, Catal. Today 35 (1997) 45.
[53] T. Fujikawa, O. Chiyoda, M. Tsukagoshi, K. Idei, S. Takehara, Catal. Today 45 (1998) 307.
[54] T. Fujikawa, O. Chiyoda, K. Idei, T. Yoshizawa, K. Usui, Stud. Surf. Sci. Catal. 121 (1999) 277.
[55] S. Zeng, J. Blanchard, M. Breysse, Y. Shi, X. Su, H. Nie, D. Li, Appl. Catal. A 298 (2006) 88.
[56] R.A. Della Betta, M. Boudart, in: J.W. Hightower (Ed.), Proceedings of the Fifth International Congress on Catalysis, North-Holland, Amsterdam, (1973), p. 1329.
[57] H.R. Reinhoudt, R. Troost, S. van Schalkwijk, A.D. van Langeveld, S.T. Sie, J.A.R. van Veen, J.A. Moulijn, Fuel Process. Technol. 61 (1999) 117.
[58] T. Matsui, M. Harada, Y. Ichihashi, K.K. Bando, N. Matsubayashi, M. Toba, Y. Yoshimura, Appl. Catal. A 286 (2005) 249.
[59] M. Guenin, M. Breysse, R. Frety, K. Tifouti, P. Marecot, J. Barbier, J. Catal. 105 (1987) 144.
[60] M. Egorova, R. Prins, J. Catal. 225 (2004) 417.